Chen et al. Nanoscale Research Letters (2015) 10:252
DOI 10.1186/s11671-015-0935-y

Nanoscale Research Letters
a SpringerOpen Journal

NANO EXPRESS Open Access

A Facile One-Pot Synthesis of Au/Cu_2O Nanocomposites for Nonenzymatic Detection of Hydrogen Peroxide

Ting Chen, Liangliang Tian*, Yuan Chen, Bitao Liu and Jin Zhang

Abstract

Au/Cu_2O nanocomposites were successfully synthesized by a facile one-pot redox reaction without additional reducing agent under room temperature. The morphologies and structures of the as-prepared products were characterized by scanning electron microscopy (SEM), transmission electron microscopy (TEM), and X-ray diffraction (XRD). The electrocatalytic performance of Au/Cu_2O nanocomposites towards hydrogen peroxide was evaluated by cyclic voltammetry (CV) and chronoamperometry (CA). The prepared Au/Cu_2O nanocomposite electrode showed a wide linear range from 25 to 11.2 mM ($R = 0.9989$) with a low detection limit of 1.05 μM ($S/N = 3$) and high sensitivity of 292.89 mA mM^{-1} cm^{-2}. The enhanced performance for H_2O_2 detection can be attributed to the introduction of Au and the synergistic effect between Au and Cu_2O. It is demonstrated that the Au/Cu_2O nanocomposites material could be a promising candidate for H_2O_2 detection.

Keywords: Au/Cu_2O nanocomposites; Nonenzymatic; Hydrogen peroxide detection

Background

In recent years, the accurate determination of H_2O_2 has attracted considerable attentions because it is an important intermediate in various fields, such as food, pharmaceutical, clinical, industrial, and environmental analyses [1–4]. Up to now, a quantity of techniques including spectrometry [5], titrimetry [6], chemiluminescence [7], and electrochemistry [8] have been developed for the quantification of H_2O_2. Among the above-mentioned techniques, electrochemical method is attractive due to its low-expense, perfect selectivity, high-sensitivity, and straightforward manipulation [9–11]. Although the enzyme-based electrochemical H_2O_2 sensors exhibit obvious advantages of high selectivity, the complicated immobilization procedure, poor stability, and high cost of the enzymes still limit their extensive applications [12, 13]. Thus, the development of enzyme-free H_2O_2 sensors with peroxidase-like activity and enhanced performance has become a trend.

Nowadays, numerous materials have been successfully applied to construct nonenzymatic H_2O_2 sensors, such as Prussian blue, noble metals, transition metal oxides, carbon nanotubes, graphene, etc [1, 14–19]. It is well known that noble metals were widely used in H_2O_2 detection and displayed excellent performance. Particularly, Au nanomaterial exhibits good catalytic activity towards the detection of H_2O_2 owing to its outstanding conductivity, electroactivity, biocompatibility and non-toxicity [20]. However, single-phase Au is too unstable to control synthesis, which suffers from difficulties such as the control of particle size, the use of stabilizing agent, and high cost. Hence, it has attracted increasing attention to Au-based nanocomposites. Up to now, Au-graphene nanosheet [21], Au-MnO_2 [22], and Au-Fe_3O_4 [23] have been reported to build H_2O_2 sensors. However, the preparation of these materials is a complicated and difficult process. Au nanoparticles were prepared by a few steps in advance and Au-based nanocomposites were obtained using various assistants under specific conditions. It is multistep, time consuming and high cost. Hence, it is essential to develop a green, environmental friendly, low-cost and efficient approach for the synthesis of Au-based nanocomposites.

Cu_2O is an important semiconductor, which is widely used in solar energy conversion, catalysis, gas sensors,

* Correspondence: tianll07@163.com
Research Institute for New Materials Technology, Chongqing University of Arts and Sciences, Yongchuan, Chongqing 402160, China

etc [24–26]. The value of Cu_2O/Cu redox pair is 0.36 V, which is much lower than that of $AuCl_4^-/Au$ (0.93 V). Consequently, Au nanoparticles can be obtained decorating onto Cu_2O through a redox reaction using Cu_2O as the reducing agent. Moreover, Cu_2O also has been reported as the electrocatalytic material for H_2O_2 detection [27, 28]. Excellent performance can be obtained by the combination of Cu_2O and Au. In this paper, Au/Cu_2O nanocomposites have been successfully prepared through a facile, one-pot, and green redox process using Cu_2O as the reducing agent. Due to the introduction of Au and the synergistic effect between Au and Cu_2O, the as-prepared product exhibited eminent performance for H_2O_2 detection. It is found that the Au/Cu_2O nanocomposite electrode exhibits high sensitivity and low detection limit towards the reduction of H_2O_2. Conclusively, with the straightforward preparation and enhanced performance of Au/Cu_2O nanocomposite electrode, the Au/Cu_2O nanocomposite material could be a promising candidate for nonenzymatic H_2O_2 sensing.

Methods

Chemicals and Materials

Chloroauric acid, dopamine (DA), uric acid (UA), and Nafion solution (5.0 wt% in a mixture of low aliphatic alcohols and water) were purchased from Sigma-Aldrich (St. Louis, MO, USA). H_2O_2 (30 wt%), $CuCl_2 \cdot 2H_2O$, NaH_2PO_4, Na_2HPO_4, ascorbic acid (AA), and glucose (Glu) were purchased from Chengdu Kelong Chemical Reagent (Chengdu, China). All the chemical reagents were of analytical grade and used as received without

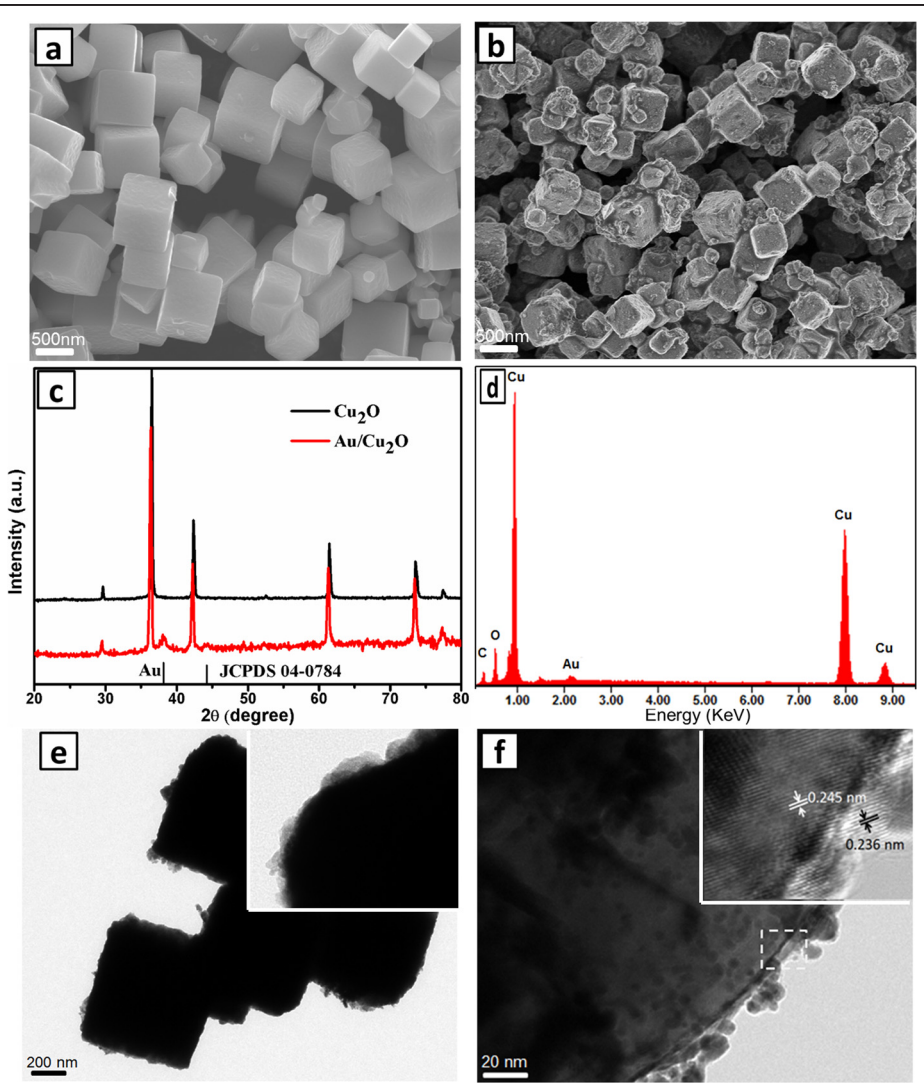

Fig. 1 SEM images of Cu_2O nanocubes (**a**) and Au/Cu_2O nanocomposites (**b**); XRD patterns of Cu_2O nanocubes and Au/Cu_2O nanocomposites (**c**); EDS (**d**), TEM image (**e**), and HRTEM image (**f**) of Au/Cu_2O nanocomposites

further purification. Ultrapure water (18.25 MΩ cm^{-1}) was used for all experiments.

Synthesis of Cubic Cu_2O

In order to prepare cubic Cu_2O, 10 mL of 2 M NaOH aqueous solution was dropped into the transparent light green $CuCl_2 \cdot 2H_2O$ aqueous solution (100 mL, 0.01 M) under vigorous stirring at 55 °C. After stirring for 0.5 h, 10 mL of 0.6 M AA solution was added into the above dark brown turbid liquid and stirred for another 3 h. Finally, the precipitates were collected by centrifugation, followed by washing thoroughly with distilled water and ethanol before freeze drying.

Synthesis of Au/Cu_2O

Au/Cu_2O nanocomposites were prepared via a one-pot, straightforward, and cost-efficient approach. Typically, 15 mg Cu_2O was dispersed in 10-mL distilled water by ultrasonic dispersion for 10 min, and then, 40-mg sodium citrate was added under constant stirring. About 15 min later, 0.5 mL of 5-mM chloroauric acid was added and the color of the solution turned into brown black immediately, implying the generation of Au nanoparticles. After 20 min, the resultant Au/Cu_2O nanocomposites were collected by centrifugation, followed by washing carefully with distilled water and ethanol before freeze drying.

Electrochemical Measurement

The modified electrode was prepared as follows: glassy carbon electrode (GCE, Φ 3) was polished with 0.3- and 0.05-μm alumina powder carefully and rinsed thoroughly with distilled water, followed by sonication in ethanol, nitric acid (1:1), and distilled water, respectively. The prepared nanocomposites were dispersed in 0.5 % Nafion ethanol solution (2 mg/mL) and ultrasonicated for 20 min. Then 5 μL of the suspension was dropped onto the surface of the polished GCE and dried in air.

All electrochemical measurements were performed on a μIII Autolab electrochemical workstation with a standard three-electrode cell in 0.1 M phosphate-buffered solution (PBS, pH = 7.0). Saturated calomel electrode (SCE) and platinum electrode were used as reference electrode and counter electrode, respectively. Cu_2O-modified GCE (Cu_2O/GCE) and Au/Cu_2O-modified GCE (Au/Cu_2O/GCE) were used as the working electrode. Cyclic voltammetry curves were obtained in the potential range from −0.60 to 0.20 V at different scan rates ranging from 20 to 160 mV/s. Chronoamperometric responses were measured at an applied potential of −0.3 V with the successive injection of different concentration of H_2O_2 per 90 s in a constant stirring system.

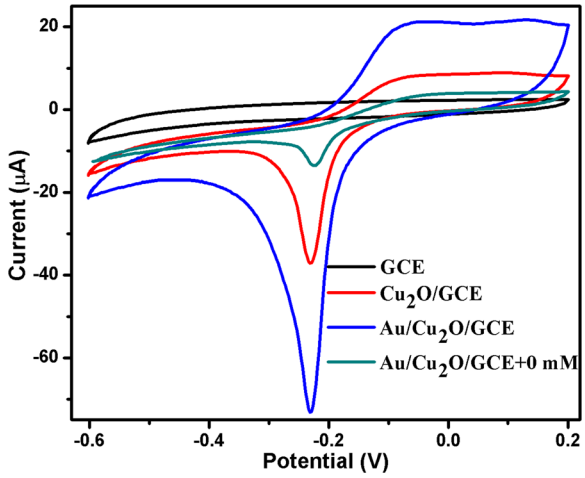

Fig. 2 CVs of different electrodes in the presence of 0.5 mM H_2O_2 in 0.1 M PBS (pH = 7.0). Scan rate: 100 mV/s

Instruments

Morphologies and structures of the prepared products were characterized by field emission scanning electron microscopy (FESEM, Hitachi, SU-8020) equipped with energy dispersion spectroscopy (EDS), transmission electron microscopy (TEM), high-resolution TEM (HRTEM) (FEI-Tecnai G2, USA), and X-ray diffraction (XRD) using Cu-Kα radiation (40 kV, 60 mA).

Results and Discussion

Characterizations

Figure 1a, b displays the SEM images of Cu_2O nanocubes and Au/Cu_2O nanocomposites. It is observed that the as-prepared cubic Cu_2O has smooth surface and relative uniform cubic shape with an average edge length of about 500 nm. Considering the fact that the Cu_2O/Cu

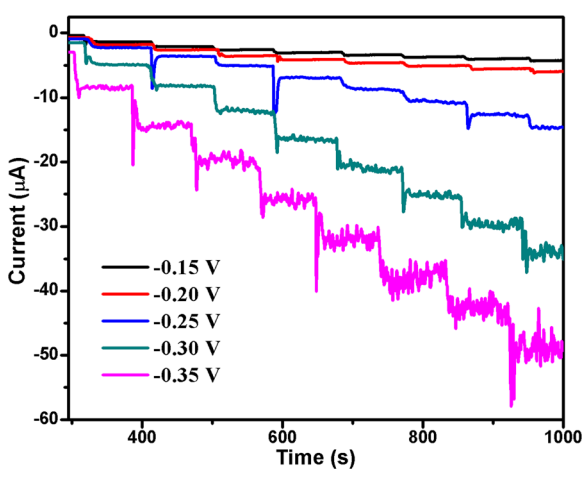

Fig. 3 Amperometric current curves of the Au/Cu_2O/GCE with the successive addition of H_2O_2 into the stirring 0.1 M PBS (pH = 7.0) at different potentials

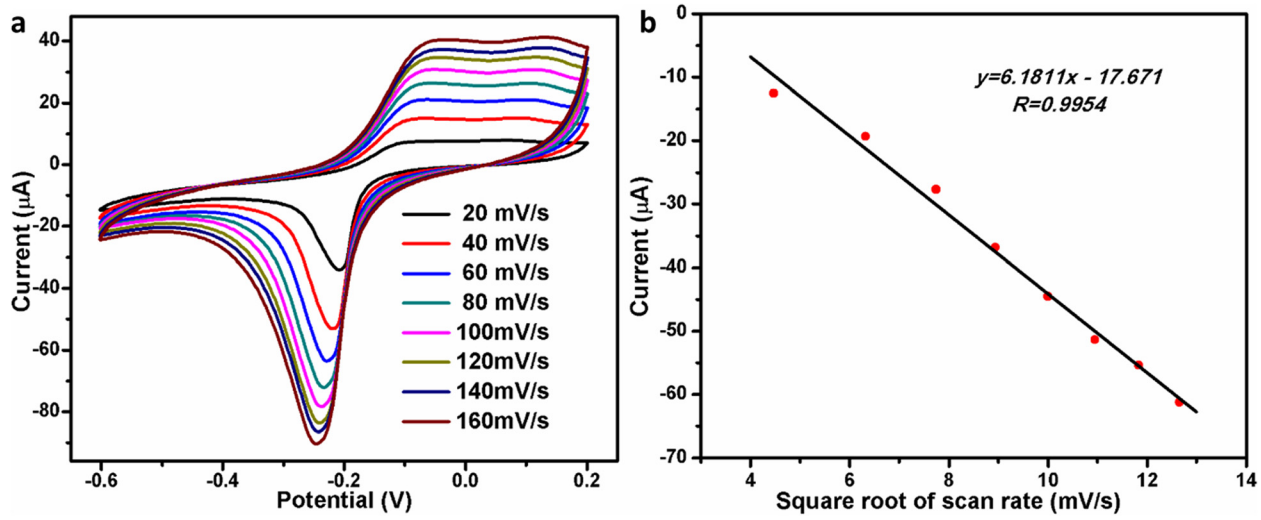

Fig. 4 **a** CVs of the Au/Cu_2O/GCE in the presence of 0.5 mM H_2O_2 at different scan rates in 0.1 M PBS (pH = 7.0). **b** The linear relationship between the cathodic current at −0.30 V and the square root of scan rates

redox pair value is 0.36 V vs. standard hydrogen electrode (SHE), which is much lower than that of $AuCl_4^-$/Au (0.93 V, vs. SHE), therefore, the in situ reduction of $AuCl_4^-$ occurs on the surface of cubic Cu_2O according to the following redox reaction [29]:

$$3Cu_2O + 2AuCl_4^- + 6H^+ = 6Cu^{2+} + 2Au + 3H_2O + 8Cl^- \quad (1)$$

It is clearly found that the surfaces of the as-prepared Au/Cu_2O nanocomposites were rough and uneven because of the generation of Au nanoparticles decorated on the surface of Cu_2O. Figure 1c shows the XRD patterns of Cu_2O nanocubes and Au/Cu_2O nanocomposites. All the diffraction peaks of Cu_2O crystal can be indexed to the standard cuprite structure (JCPDS 05-0667). Compared with the Cu_2O diffraction pattern, two additional peaks located at about 38.2° and 44.3° were observed, which were assigned to the (111) and (200) diffraction peaks of Au (JCPDS 04-0784). In addition, the EDS spectrum (Fig. 1d) confirms the presence of Au, Cu, and O elements, which agrees with the XRD spectrum analysis. Figure 1e shows the TEM image of Au/Cu_2O nanocomposites, and it is found that Au/Cu_2O nanocomposites with defined cubic shapes were distinctly decorated by Au nanoparticles. Furthermore, HRTEM image (Fig. 1f) clearly shows that Au nanoparticles homogeneously distribute on the surface of Cu_2O cubes and the particle size of Au is about 3 nm. It is observed that the spacing of marked adjacent lattice fringes are about 0.236 and 0.245 nm, which is consistent with the standard value of Au (111) and Cu_2O (111), respectively. The result is in accordance with the XRD spectrum analysis. The formation of the Au/Cu_2O heterostructures may be attributed to the similar (111) lattice spacing of Au and Cu_2O, which forced Au heterogeneous nucleation on the surfaces of Cu_2O cubes.

Electrochemical Performance of Au/Cu_2O/GCE

Au/Cu_2O/GCE was constructed to research the electrochemical performance towards the reduction of H_2O_2. Figure 2 shows the electrocatalytic responses of bare GCE, Cu_2O/GCE, and Au/Cu_2O/GCE in the presence of 0.5 mM H_2O_2 in 0.1 M PBS solution (pH = 7.0). It is found that no reduction peak is observed on bare GCE with the injection of H_2O_2 into the PBS solution. Apparently, Cu_2O/GCE shows a significant reduction peak towards the reduction of H_2O_2. It may be ascribed to the

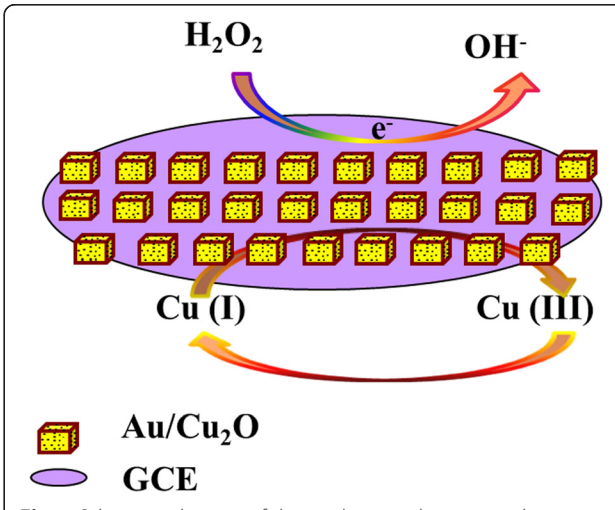

Fig. 5 Schematic diagram of the catalytic mechanism on the Au/Cu_2O/GCE for H_2O_2 reduction

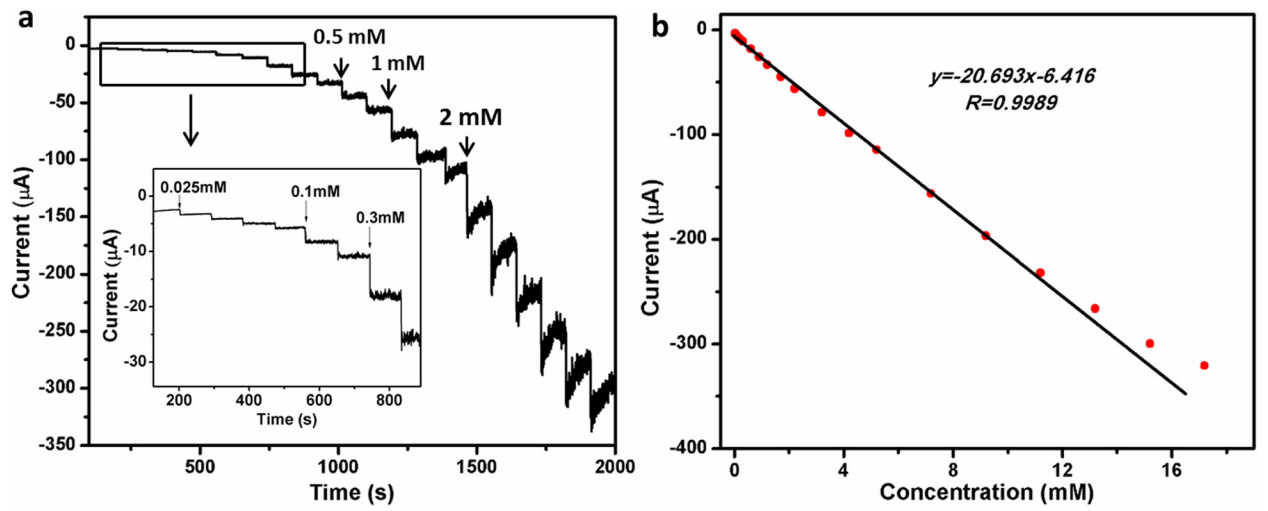

Fig. 6 a Amperometric current curve of the Au/Cu_2O/GCE with the successive addition of H_2O_2 into the stirring 0.1 M PBS (pH = 7.0) at −0.3 V. Inset is the amplification of the marked rectangle region shown in the curve. **b** The linear relationship between the catalytic current and the concentration of H_2O_2

fact that Cu^{I} species turned into Cu^{III} species, which is in agreement with the previous reports [30]. Notably, the reduction peak current of H_2O_2 on the Au/Cu_2O/GCE is further increased. It is also important to show that the Au/Cu_2O/GCE exhibits a quite weak electrochemistry response in the absence of H_2O_2. All these observations indicate that Au/Cu_2O nanocomposites exhibit notable electrocatalytic activity towards the reduction of H_2O_2. The excellent activity can be ascribed to the faster electron transfer kinetics, which is caused by the increase of electroactive area and the electron transfer rate. In addition, different work function between Au nanoparticle and Cu_2O semiconductor leads to the charge redistribution at the interfaces of Au/Cu_2O nanocomposites [31]. The redistribution of the surface charges may improve the electrocatalytic activity [32]. Comprehensively, the improved catalytic activity for H_2O_2 reduction is caused by the introduction of Au and the synergistic effect between Au and Cu_2O, which is in agreement with the previous reports [22, 23].

In order to obtain the optimal response to H_2O_2, the effect of applied potential on the response current was investigated. Figure 3 shows the amperometric current curves of the Au/Cu_2O/GCE with the successive addition of 0.1 mM H_2O_2 into 0.1 M PBS (pH = 7.0) at different potentials from −0.15 to −0.35 V. It is found that the current response of −0.15, −0.20, and −0.25 V are lower than that of −0.30 and −0.35 V. Compared with the potential of −0.30 V, the response current of −0.35 V is less stable and has larger background noise. In addition, some interfering species which are stable under relatively

Table 1 Comparison of H_2O_2 determination of different modified electrodes

Electrode	Linear range (μM)	Limit of detection (μM)	Reference
Cu_2O MCs[a]	5–1500	1.5	[34]
Cu_2O HNs[b]	2–150	1.03	[35]
Cu_2O/GNs[c]	300–7800	20.8	[36]
Au NPs[d]	100–50,000	4.0	[37]
Ag-Au-rGO	100–5000	1.0	[38]
Au/Cu_2O NCs[e]	25–11,200	1.05	this work

[a]Cu_2O microcubes, [b]Cu_2O hollow nanocubes, [c]Cu_2O nanocubes wrapped by graphene nanosheets, [d]Au nanoplates, [e]Au/Cu_2O nanocomposites

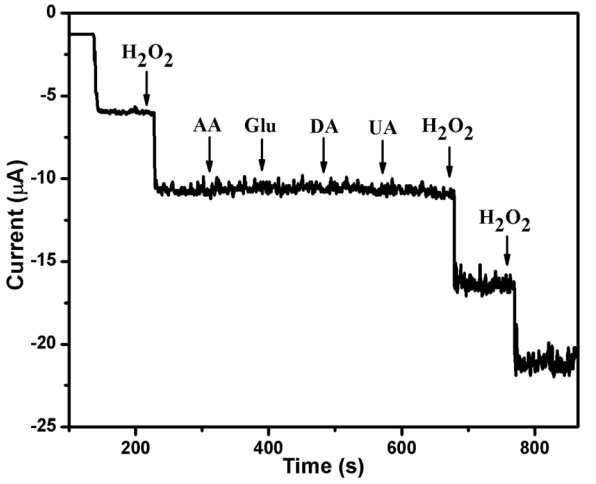

Fig. 7 Amperometric current curve of Au/Cu_2O/GCE with the successive addition of a 0.2 mM concentration of H_2O_2, AA, Glu, DA, and UA

low potential would be oxidized at high potential [33]. Thus, −0.30 V was chosen as the working potential for the detection of H_2O_2.

To further investigate the electrode kinetic process, the cyclic voltammetries (CVs) of Au/Cu_2O/GCE at different scan rates were also examined. As shown in Fig. 4, the reduction peak current increases linearly with the square root of the scan rates ($v^{1/2}$) in the range of 20 to 160 mV/s ($R = 0.9954$). The result indicates that the electron transfer of Au/Cu_2O nanocomposites on the GCE is a diffusion-controlled electrochemical process. Comprehensively, a proposed catalytic mechanism for the reduction of H_2O_2 on the Au/Cu_2O/GCE was displayed in Fig. 5. Cu^{I} turned into Cu^{III} species providing electrons to the reduction of H_2O_2, and meanwhile, Au accelerated electron transfer kinetics in the electroactive surface area.

Amperometric Detection of H_2O_2 at Au/Cu_2O/GCE

To quantify the electrochemical detection of H_2O_2, the Au/Cu_2O/GCE was evaluated by chronoamperometry (CA). Figure 6a depicts the amperometric current curve of Au/Cu_2O/GCE at an applied potential of −0.30 V with the successive injection of different concentrations of H_2O_2 into PBS (pH = 7.0). The inset of Fig. 6a is a magnified current-time curve at low concentrations. It shows a stepwise increase in agreement with H_2O_2 addition and reaches a steady status within 3 s. Figure 6b depicts the linear relationship between catalytic currents and H_2O_2 concentrations. The Au/Cu_2O/GCE for H_2O_2 detection shows a wide linear range from 25 μM to 11.2 mM with a lower detection limit of 1.05 μM ($S/N = 3$) and high sensitivity of 292.89 μA mM^{-1} cm^{-2}. The linear regression equation is $y = -20.693x - 6.416$ [y(μA); x(mM)] with a correlation coefficient of $R = 0.9989$. Above all, Au/Cu_2O/GCE exhibited excellent performance towards the reduction of H_2O_2. The enhanced electrocatalytic performance could be ascribed to the outstanding conductivity and electroactivity of Au nanoparticles, which accelerates the transfer rate of electrons in the reduction of H_2O_2. Table 1 shows the comparison of H_2O_2 determination of different modified electrodes. It is shown that Au/Cu_2O nanocomposites exhibited a wider linear range and lower detection limit towards the detection of H_2O_2.

Interference and Stability Study

To investigate the selectivity of the Au/Cu_2O/GCE towards H_2O_2, several possible interfering species were examined. Figure 7 shows the amperometric response with the successive injection of 0.2 mM H_2O_2 and 0.2 mM interfering species, including AA, Glu, DA, and UA at an applied potential of −0.30 V in PBS (pH = 7.0). Apparently, no interference current is found in the testing process indicating the excellent selectivity of Au/Cu_2O/GCE towards H_2O_2. The stability of Au/Cu_2O/GCE was evaluated by the current step method measuring the amperometric current responses towards 1 mM H_2O_2 repeating ten times, and it is found that the relative standard deviation (RSD) was approximately 1.3 %. In addition, the amperometric current response to H_2O_2 over a long operational period of 1500 s was about 95 % of its original counterpart. These observations indicate that the Au/Cu_2O/GCE is relatively stable.

Conclusions

Au/Cu_2O nanocomposites were successfully synthesized by a facile one-pot green redox reaction using Cu_2O as the reducing agent. The Au/Cu_2O/GCE exhibited excellent performance for nonenzymatic detection of H_2O_2 with high selectivity, low detection limit, and strong anti-interference capability. The excellent electrocatalytic activity may be caused by the introduction of Au and the synergistic effect between Au and Cu_2O. The Au/Cu_2O nanocomposite material is promising for practical applications in nonenzymatic detection of H_2O_2.

Competing interests

The authors declare that they have no competing interests.

Authors' contributions

TC carried out the experiment and wrote the paper. LT designed the experiment and gave revise for the grammar of the manuscript. YC and BL prepared the solution. JZ did the electrochemical measurement. All authors read and approved the final manuscript.

Acknowledgements

This study is supported by the National Natural Science Foundation of China (21403020, 21401015), the Basic and Frontier Research Program of Chongqing Municipality (cstc2014jcyjA50012), and the Foundation of Chongqing University of Arts and Sciences (Z2011XC15).

Received: 10 April 2015 Accepted: 13 May 2015
Published online: 03 June 2015

References

1. Zhou M, Zhai YM, Dong SJ. Electrochemical sensing and biosensing platform based on chemically reduced graphene oxide. Anal Chem. 2009;81:5603–13.
2. Xiao Y, Ju HX, Chen HY. Hydrogen peroxide sensor based on horseradish peroxidase-labeled Au colloids immobilized on gold electrode surface by cysteamine monolayer. Anal Chim Acta. 1999;391:73–82.
3. Yamamoto K, Shi GY, Zhou TS, Xu F, Xu JM, Kato T, et al. Study of carbon nanotubes-HRP modified electrode and its application for novel on-line biosensors. Analyst. 2003;3:249–54.
4. Hrapovic S, Liu Y, Male KB, Luong JH. Electrochemical biosensing platforms using platinum nanoparticles and carbon nanotubes. Anal Chem. 2004;76:1083–8.
5. Matsubara C, Kawamoto N, Takamura K. Oxo [5,10,15,20-tetra(4-pyridyl) porphyrinato]titanium(IV): an ultra-high sensitivity spectrophotometric reagent for hydrogen peroxide. Analyst. 1992;117:1781–4.
6. Hurdis EC, Romeyn H. Accuracy of determination of hydrogen peroxide by cerate oxidimetry. Anal Chem. 1954;26:320–5.
7. Greenway GM, Leelasattarathkul T, Liawruangrath S, Wheatley RA, Youngvises N. Ultrasound-enhanced flow injection chemiluminescence for determination of hydrogen peroxide. Analyst. 2006;131:501–8.

8. Xi FN, Zhao DJ, Wang XW, Chen P. Non-enzymatic detection of hydrogen peroxide using a functionalized three-dimensional graphene electrode. Electrochem Commun. 2013;26:81–4.
9. Tang N, Zheng JB, Sheng QL, Zhang HF, Liu RX. A novel H_2O_2 sensor based on the enzymatically induced deposition of polyaniline at a horseradish peroxide/aligned single-wall carbon nanotubes modified Au electrode. Analyst. 2011;136:781–6.
10. Li J, Qiu JD, Xu JJ, Chen HY, Xia XH. The synergistic effect of Prussian-blue-grafted carbon nanotube-poly(4-vinylpyridine) composites for amperometric sensing-AFM. Adv Funct Mater. 2007;17:1574–80.
11. Chen SH, Yuan R, Chai YQ, Zhang LY, Wang N, Li XL. Amperometric third-generation hydrogen peroxide biosensor based on the immobilization of hemoglobin on multiwall carbon nanotubes and gold colloidal nanoparticles. Biosens Bioelectron. 2007;22:1268–74.
12. Lu XB, Zhang Q, Zhang L, Li JH. Direct electron transfer of horseradish peroxidase and its biosensor based on chitosan and room temperature ionic liquid. Electrochem Commun. 2006;8:874–8.
13. Xu Q, Mao C, Liu NN, Zhu JJ, Sheng J. Direct electrochemistry of horseradish peroxidase based on biocompatible carboxymethyl chitosan-gold nanoparticle nanocomposite. Biosens Bioelectron. 2006;22:768–73.
14. Jin E, Lu XF, Cui LL, Chao DM, Wang C. Fabrication of graphene/Prussian blue composite nanosheets and their electrocatalytic reduction of H_2O_2. Electrochimica Acta. 2010;55:7230–4.
15. Welch CM, Banks CE, Simm AO, Compton RG. Silver nanoparticle assemblies supported on glassy-carbon electrodes for the electro-analytical detection of hydrogen peroxide. Anal Bioanal Chem. 2005;382:12–21.
16. Li XY, Liu YX, Zheng LC, Dong MJ, Xue ZH, Lu XQ, et al. A novel nonenzymatic hydrogen peroxide sensor based on silver nanoparticles and ionic liquid functionalized multiwalled carbon nanotube composite modified electrode. Electrochim Acta. 2013;113:170–5.
17. Yan Q, Wang ZL, Zhang J, Peng H, Chen XJ, Hou HN, et al. Nickel hydroxide modified silicon nanowires electrode for hydrogen peroxide sensor applications. Electrochim Acta. 2012;66:148–53.
18. Yang PH, Wei WZ, Tao CY, Xie BH, Chen XY. Nano-silver/multi-walled carbon nanotube composite films for hydrogen peroxide electroanalysis. Microchim Acta. 2008;162:51–6.
19. Kang XH, Mai ZB, Zou XY, Cai PX, Mo JY. Glucose biosensors based on platinum nanoparticles-deposited carbon nanotubes in sol-gel chitosan/silica hybrid. Talanta. 2008;74:879–95.
20. Jain PK, Huang X, El-Sayed IH, El-Sayed MA. Noble metals on the nanoscale: optical and photothermal properties and applications in imaging, sensing, biology and medicine. Acc Chem Res. 2008;41:1578–86.
21. Fang YX, Guo SJ, Zhu CZ, Zhai YM, Wang EK. Self-assembly of cationic polyelectrolyte-functionalized graphene nanosheets and gold nanoparticles a two-dimensional heterostructure for hydrogen peroxide sensing. Langmuir. 2010;26:11277–82.
22. Li YL, Zhang J, Zhu H, Yang F, Yang XR. Gold nanoparticles mediate the assembly of manganese dioxide nanoparticles for H_2O_2 amperometric sensing. Electrochimica Acta. 2010;55:5123–8.
23. Lee Y, Garcia MA, Huls NAF, Sun S. Synthetic tuning of the catalytic properties of Au-Fe_3O_4 nanoparticles. Angew Chem. 2010;49:1271–4.
24. Deng S, Tjoa V, Fan HM, Tan HR, Sayle DC, Olivo M, et al. Reduced graphene oxide conjugated Cu_2O nanowire mesocrystals for high-performance NO_2 gas sensor. J Am Chem Soc. 2012;134:4905–17.
25. Huang WC, Lyu LM, Yang YC, Huang MH. Synthesis of Cu_2O nanocrystals from cubic to rhombic dodecahedral structures and their comparative photocatalytic activity. J Am Chem Soc. 2012;134:1261–7.
26. Jayatissa H, Samarasekara P, Kun G. Methane gas sensor application of cuprous oxide synthesized by thermal oxidation. Phys Status Solidi A. 2009;206:332–7.
27. Li S, Zheng YJ, Qin GW, Ren YP, Pei WL, Zuo L. Enzyme-free amperometric sensing of hydrogen peroxide and glucose at a hierarchical Cu_2O modified electrode. Talanta. 2011;85:1260–4.
28. Yan ZK, Zhao JW, Qin LR, Mu F, Wang P, Feng XN. Non-enzymatic hydrogen peroxide sensor based on a gold electrode modified with granular cuprous oxide nanowires. Microchim Acta. 2013;180:145–50.
29. Millazzo G, Caroli S. Tables of standard electrode potentials. 26th ed. New York: John Wiley & Sons; 1978. p. 661.
30. Prathap MU, Kaur B, Srivastava R. Hydrothermal synthesis of CuO micro-/nanostructures and their applications in the oxidative degradation of methylene blue and non-enzymatic sensing of glucose/H_2O_2. J Colloid Inter Sci. 2012;370:144–54.
31. Wang XD, Summers CJ, Wang ZL. Self-attraction among aligned Au/ZnO nanorods under electron beam. Appl Phys Lett. 2005;86:013111–21.
32. Hua QY, Wang FY, Fang Z, Liu XW. Cu_2O-Au nanocomposites for enzyme-free glucose sensing with enhanced performances. Colloid Surf B. 2012;95:279–83.
33. Luo BB, Li XM, Yang JC, Li XL, Xue LP, Gu JK, et al. Non-enzymatic electrochemical sensors for the detection of hydrogen peroxide based on Cu_2O/Cu nanocomposites. Anal Methods. 2014;6:1114–20.
34. Zhang L, Li H, Ni YH, Li J, Liao KM, Zhao GC. Porous cuprous oxide microcubes for non-enzymatic amperometric hydrogen peroxide and glucose sensing. Electrochem Commun. 2009;11:812–5.
35. Gao ZY, Liu JL, Chang JL, Wu DP, He JJ, Wang K, et al. Mesocrystalline Cu_2O hollow nanocubes: synthesis and application in non-enzymatic amperometric detection of hydrogen peroxide and glucose. CrystEngComm. 2012;14:6639–46.
36. Liu MM, Liu R, Chen W. Graphene wrapped Cu_2O nanocubes: non-enzymatic electrochemical sensors for the detection of glucose and hydrogen peroxide with enhanced stability. Biosens Bioelectron. 2013;45:206–12.
37. Ning R, Lu WB, Zhang YW, Qin XY, Luo YL, Hu JM, et al. A novel strategy to synthesize Au nanoplates and their application for enzymeless H_2O_2 detection. Electrochimica Acta. 2012;60:13–6.
38. Kumar GG, Babu KJ, Nahm KS, Hwang YJ. A facile one-pot green synthesis of reduced graphene oxide and its composites for nonenzymatic hydrogen peroxide sensor applications. Rsc Adv. 2014;4:7944–51.